



Biological and Structural Properties of Wild-Type and Mutant Mengoviruses
by KEVIN ANDERSON

A thesis submitted in partial fulfillment of the requirements for the degree of Doctor of Philosophy
Microbiology

Montana State University

© Copyright by KEVIN ANDERSON (1984)

Abstract:

Mechanisms for the interaction- of mengovirus with human erythrocytes, cultured cells, and mice were examined. Agglutination of human erythrocytes by mengovirus was dependent on the presence of sialic acid on the erythrocyte surface. However, free sialic acid failed to inhibit hemagglutination. Glycophorin, the major sialoglycoprotein of human erythrocyte membranes, exhibited receptor specificity for the mengovirus. Cross-linking studies indicated that the alpha (1D) structural protein of mengovirus bound specifically to glycophorin. Biological and structural properties of two mutants of mengovirus, 205 and 280, were compared to those of wild-type virus to understand virus-cell interactions at the molecular level. The mutants exhibited alterations in plaque morphology, hemagglutination, and virulence in mice, but were not temperature-sensitive. Wild-type mengovirus exhibited LD₅₀ titers of 7 and 1500 plaque forming units (PFU) in mice infected intracranially (IC) and intraperitoneally (IP), respectively. Mice infected IC or IP with up to 10⁷ PFU of mutants 205 and 280 showed no symptoms of mengovirus infection. Revertants were isolated from the brains of mice infected with mutant 205 and characterized. The results suggest that hemagglutination and virulence are phenotypically linked traits. Reduction in the amount of virus-specified protein and RNA synthesis in BHK-21 cells infected by the mutants may be due to an alteration in the binding affinities of the mutants. The degree of virulence in mice and the size of plaques produced by mengovirus isolates may also be dependent upon binding affinity for cells. Analysis of surface- and metabolically-labeled structural proteins by SDS-PAGE failed to detect any gross differences among the wild-type and mutant viruses. Peptide analysis by two-dimensional thin layer chromatography and high performance liquid chromatography suggested that extensive structural homology exists among the proteins of wild-type and mutant viruses. Two dimensional gel electrophoresis of wild-type and mutant structural proteins revealed alterations in the isoelectric character of the alpha (1D) protein of both mutant 205 1D) protein were responsible for the phenotypic changes expressed by the mutants.

BIOLOGICAL AND STRUCTURAL PROPERTIES OF
WILD-TYPE AND MUTANT MENGOVIRUSES

by

Kevin Anderson

A thesis submitted in partial fulfillment
of the requirements for the degree

of

Doctor of Philosophy

in

Microbiology

MONTANA STATE UNIVERSITY
Bozeman, Montana

November 1984

D378
AN 235
Cop. 2

APPROVAL

of a thesis submitted by

Kevin Anderson

This thesis has been read by each member of the thesis committee and has been found to be satisfactory regarding content, English usage, format, citations, bibliographic style, and consistency, and is ready for submission to the College of Graduate Studies.

11-20-84
Date

[Signature]
Chairperson, Graduate Committee

Approved for the Major Department

11-20-84
Date

Norman H. Reed
Head, Major Department

Approved for the College of Graduate Studies

11-20-84
Date

MP Malone
Graduate Dean

STATEMENT OF PERMISSION TO USE

In presenting this thesis in partial fulfillment of the requirements for a doctoral degree at Montana State University, I agree that the Library shall make it available to borrowers under the rules of the Library. I further agree that the copying of this thesis is allowable only for scholarly purposes, consistent with "fair use" as prescribed in the U.S. Copyright Law. Requests for extensive copying or reproduction of this thesis should be referred to University Microfilms International, 300 North Zeeb Road, Ann Arbor, Michigan 48106, to whom I have granted "the exclusive right to reproduce and distribute copies of the dissertation in and from microfilm and the right to reproduce and distribute by abstract in any format."

Signature



Date

9-4-84

TABLE OF CONTENTS

	Page
LIST OF TABLES.....	vi
LIST OF FIGURES.....	viii
ABSTRACT.....	x
INTRODUCTION.....	1
Classification.....	2
Physical and Chemical Properties.....	3
Protein Processing and Assembly of Virus Particles.....	6
Structure of the Virion.....	8
Pathogenic Properties.....	10
Virus-Cell Interactions and Receptor Studies...	12
Biological and Biochemical Properties of Plaque Variants.....	13
Temperature Sensitive Mutants of Mengovirus....	15
 MATERIALS AND METHODS.....	 20
Chemicals and Reagents.....	20
Virus Strains.....	20
Cell Lines.....	21
Plaque Assay.....	22
Infection and Purification.....	23
Radiolabeling of Virus-Specified Proteins.....	24
Radiolabeling of Virus-Specified RNA.....	27
Hemagglutination Assays.....	28
Glycophorin Purification and Cross-linking.....	29
SDS-Polyacrylamide Gel Electrophoresis.....	32
Two-Dimensional Gel Electrophoresis.....	34
Enzymatic Digestion.....	35
Peptide Analysis.....	36
Infection of Mice.....	37
Production of Hyperimmune Ascitic Fluid.....	37
Immunofluorescence Assay.....	38
Plaque Neutralization.....	38
Determination of Particle:PFU Ratios.....	39
Adsorption of Viruses to BHK-21 Cells.....	39

TABLE OF CONTENTS (continued)

	Page
RESULTS:.....	41
Temperature-Sensitivity and Plaque Size.....	41
Hemagglutination.....	44
Mechanism of Hemagglutination.....	45
Virus Multiplication in Mouse Cell Lines.....	58
Virulence in BALB/c Mice.....	59
Plaque Neutralization.....	67
Comparative Analysis of Mengovirus Structural Proteins.....	69
Synthesis of Virus-Specified Intracellular Protein and RNA.....	91
Adsorption of Virus to BHK-21 Cells.....	96
Particle:PFU Ratios.....	97
DISCUSSION.....	100
Temperature-Sensitivity and Plaque Morphology.	100
Virulence in Mice.....	104
Mechanism of Mengovirus Hemagglutination.....	107
Structural Properties of the Mutant and Wild-Type Viruses.....	110
Revertant Studies.....	113
Physiological Effects of Mutation.....	116
Conclusions.....	117
LITERATURE CITED.....	118
APPENDICES.....	127
Bradford Protein Assay of Fetuin.....	128
SDS-PAGE of Electroeluted Structural Proteins of Mengovirus Mutants 205 and 280.....	129
Discontinuous Linear Gradient for HPLC Analysis of Tryptic Peptides.....	130
Calculations for Determining the Particle:PFU Ratios for Wild-Type and Mutant Mengoviruses..	131

LIST OF TABLES

Table	Page
1. Characterization of temperature-sensitive mutants of mengovirus with respect to RNA synthesis and hemagglutination.....	18
2. Temperature-sensitivity of mengovirus mutants as a function of yield.....	42
3. Mean plaque diameters of wild-type and mutant mengoviruses.....	43
4. Hemagglutination assay of wild-type and mutant mengoviruses.....	45
5. Effect of neuraminidase-treatment of human type O erythrocytes on mengovirus hemagglutination...	46
6. List of carbohydrates tested as inhibitors of mengovirus hemagglutination.....	47
7. Multiplication of wild-type and mutant mengoviruses in mouse cell lines.....	59
8. LD ₅₀ titers for wild-type and mutant mengoviruses in BALB/c mice following intraperitoneal infection.....	60
9. LD ₅₀ titers for wild-type and mutant mengoviruses in BALB/c mice following intracranial infection.....	61
10. Effect of brain suspension on the infectivity of wild-type and mutant mengoviruses.....	63
11. Yield of wild-type and mutant mengoviruses in BALB/c mouse brains following intracranial or intraperitoneal infection.....	64
12. Hemagglutination assay of plaque isolates from brain suspensions of BALB/c mice infected with wild-type or mutant mengoviruses.....	66

LIST OF TABLES (continued)

Table	Page
13. Further characterization of the cloned plaque isolates from brain homogenates of mice infected intracranially with mutant 205.....	67
14. Plaque neutralization titers of the mengovirus-specific hyperimmune ascitic fluid for the wild-type, mutant, and revertant viruses.....	70
15. Adsorption of wild-type, mutant and revertant viruses to BHK-21 cells.....	98
16. Calculations for determining the particle:PFU ratios for wild-type and mutant mengoviruses....	131

LIST OF FIGURES

Figure	Page
1. A model of the mengovirus capsid.....	5
2. A diagram showing the generation of the capsid polypeptides of mengovirus.....	7
3. Mechanism of cross-linkage of glycophorin to mengovirus.....	31
4. Densitometer tracings of purified glycophorin analyzed by SDS-PAGE.....	50
5. Effect of glycophorin on the migration of purified mengovirus in sucrose density gradients.....	52
6. Effect of glycophorin on the migration of purified wild-type and mutant mengoviruses in sucrose density gradients.....	53
7. SDS-PAGE of the structural proteins of purified wild-type mengovirus cross-linked to glycophorin.....	56
8. Densitometer tracings of the mengovirus structural proteins cross-linked to glycophorin.....	57
9. SDS-PAGE of ¹⁴ C-labeled wild-type and mutant mengovirus structural proteins.....	72
10. HPLC analysis of ³⁵ S-methionine-labeled tryptic peptides of the delta (1A) proteins of wild-type and mutant mengoviruses.....	74
11. HPLC analysis of ³⁵ S-methionine-labeled tryptic peptides of the beta (1B) proteins of wild-type and mutant mengoviruses.....	75
12. HPLC analysis of ³⁵ S-methionine-labeled tryptic peptides of the gamma (1C) proteins of wild-type and mutant mengoviruses.....	76

LIST OF FIGURES (continued)

Figure	Page
13. HPLC analysis of ^{35}S -methionine-labeled tryptic peptides of the alpha (1D) proteins of wild-type and mutant mengoviruses.....	77
14. SDS-PAGE of ^{125}I -labeled proteins of intact wild-type and mutant mengovirus particles.....	80
15. Two-dimensional analysis of ^{125}I -labeled chymotryptic peptides of the alpha (1D) proteins of wild-type and mutant mengoviruses..	83
16. Two-dimensional IEF gel electrophoresis of ^{35}S -methionine-labeled structural proteins of wild-type, mutant, and revertant mengoviruses..	85
17. Two-dimensional IEF gel electrophoresis of ^{35}S -methionine mixed samples of the structural proteins of the wild-type, mutant, and revertant mengoviruses.....	88
18. Two-dimensional NEPHGE gel electrophoresis of ^{35}S -methionine-labeled structural proteins wild-type, mutant, and revertant mengoviruses..	91
19. Time course for mengovirus-specified protein synthesis in wild-type-, mutant 205-, and mutant 280-infected cells.....	95
20. Time course for mengovirus-specified RNA synthesis in wild-type-, mutant-, and revertant-infected cells.....	96
21. Bradford protein assay of fetuin.....	128
22. SDS-PAGE of electroeluted structural proteins of mengovirus mutants 205 and 280.....	129
23. Discontinuous linear gradient for HPLC analysis of tryptic peptides.....	130

ABSTRACT

Mechanisms for the interaction of mengovirus with human erythrocytes, cultured cells, and mice were examined. Agglutination of human erythrocytes by mengovirus was dependent on the presence of sialic acid on the erythrocyte surface. However, free sialic acid failed to inhibit hemagglutination. Glycophorin, the major sialoglycoprotein of human erythrocyte membranes, exhibited receptor specificity for the mengovirus. Cross-linking studies indicated that the alpha (1D) structural protein of mengovirus bound specifically to glycophorin. Biological and structural properties of two mutants of mengovirus, 205 and 280, were compared to those of wild-type virus to understand virus-cell interactions at the molecular level. The mutants exhibited alterations in plaque morphology, hemagglutination, and virulence in mice, but were not temperature-sensitive. Wild-type mengovirus exhibited LD₅₀ titers of 7 and 1500 plaque forming units (PFU) in mice infected intracranially (IC) and intraperitoneally (IP), respectively. Mice infected IC or IP with up to 10⁷ PFU of mutants 205 and 280 showed no symptoms of mengovirus infection. Revertants were isolated from the brains of mice infected with mutant 205 and characterized. The results suggest that hemagglutination and virulence are phenotypically linked traits. Reduction in the amount of virus-specified protein and RNA synthesis in BHK-21 cells infected by the mutants may be due to an alteration in the binding affinities of the mutants. The degree of virulence in mice and the size of plaques produced by mengovirus isolates may also be dependent upon binding affinity for cells. Analysis of surface- and metabolically-labeled structural proteins by SDS-PAGE failed to detect any gross differences among the wild-type and mutant viruses. Peptide analysis by two-dimensional thin layer chromatography and high performance liquid chromatography suggested that extensive structural homology exists among the proteins of wild-type and mutant viruses. Two dimensional gel electrophoresis of wild-type and mutant structural proteins revealed alterations in the isoelectric character of the alpha (1D) protein of both mutant 205 and 280. These data suggest that alterations in the alpha (1D) protein were responsible for the phenotypic changes expressed by the mutants.

INTRODUCTION

Advancement of our knowledge of the function and organization of biological systems has been obtained in part through the generation and characterization of mutants. Mutants may arise as a result of physical or chemical modification of genetic information. This may occur spontaneously or by the use of known mutagenic agents. Mutants which arise from single mutations and express stable phenotypic characters are particularly useful in genetic studies. They provide a means of identifying the biological functions of specific gene products. Genetic maps specifying the location of genes or gene families coding for specific gene products may be ascertained by mutant characterization.

Mengovirus, a neurotropic picornavirus, contains a limited amount of genetic material and provides a relatively simple system for the study of virus-host interactions. Mutants of mengovirus have been isolated to gain an understanding of the biological functions of the virus and to assign these functions to specific genes. Two temperature-sensitive mutants of mengovirus were isolated which lack the ability to agglutinate human type O erythrocytes (Dr. M. A. Gill, personal communication).

Further characterization of the biological and biochemical properties of these mutants should provide a means of understanding the mechanism of mengovirus hemagglutination as well as other biological functions which differ from those of the wild-type virus as a result of the expression of altered phenotypic characters.

Classification

Mengovirus is a member of the picornaviridae, which comprise a diverse group of small (pico), RNA-containing (RNA) viruses. Picornaviruses are classified into five distinct groups or genera, based on buoyant density in CsCl gradients, acid lability, and viral serology (66). The enteroviruses, which include the polioviruses, are stable in the acid pH range and have a density of 1.34 g/ml in cesium chloride gradients. The cardioviruses, which include encephalomyocarditis (EMC) virus and mengovirus, share the same buoyant density in cesium chloride with the enteroviruses, but are unrelated serologically. The rhinoviruses and aphthoviruses have different buoyant densities in cesium chloride gradients (1.40 and 1.44 g/ml, respectively) than the enteroviruses and cardioviruses and are unstable in the acid pH range. A fifth group, comprising picornavirus-like agents, includes Hepatitis A virus. No common intergeneric antigens have been described.

Physical and Chemical Properties

The mengovirus particle is composed of a single RNA molecule surrounded by an icosahedral protein capsid (49,83). It has a dry diameter of 27-28 nm, is composed of 70% protein and 30% RNA by weight, and has a molecular weight of 8.5×10^6 (71). No lipid or carbohydrate molecules are associated with the virus particle (10).

The RNA molecule is single stranded and has a molecular weight of $2.4-2.7 \times 10^6$ (83). The 3' end of the RNA molecule is polyadenylated. Polyadenylation is required for infectivity of the RNA molecule (36). A polycytidylate-rich region is located near the 5' end of the RNA molecule (65). The function and evolutionary significance of this region is unknown. A small protein, VPg (3B)¹, is covalently linked to the 5' end (37). This protein is not necessary for infectivity of the RNA molecule (57) and is thought to be involved in RNA replication and the assembly of virions (58).

The capsid is composed of four major proteins: alpha (1D), 37 kilodaltons (kd); beta (1B), 33 kd; gamma (1C), 25 kd; and delta (1A), 7.8 kd (5,11,83). There are 60 copies of each protein in a complete capsid (5,69). Together the 4 major structural proteins form one subunit

¹ The recently adopted convention for the nomenclature of picornavirus proteins (70) is shown in parentheses.

and there are 60 subunits per capsid. A model of the mengovirus capsid is shown in Figure 1.

Four minor polypeptides have been identified in association with the mengovirus capsid: epsilon (1AB), 40 kd (5,83); D1 (1ABC), 69 kd (5); D2 (1CD), 59 kd (5,83); and beta' (1B'), 29 kd (5). Epsilon (1AB), D1 (1ABC), and D2 (1CD) are uncleaved precursors of the major capsid proteins. Two polypeptides of the epsilon (1AB) protein are found per capsid (5,83). D1 (1ABC), D2 (1CD), and beta' (1B') are found only in virions produced at 31.5°C (5). Approximately two copies each of the D1 (1ABC) and D2 (1CD) proteins are found per capsid. The beta' (1B') protein is thought to arise from an alteration in the cleavage which produces the beta (1B) protein (5). Wild-type virions produced at 31.5°C contain approximately 7 beta' (1B') and 53 beta (1B) polypeptides per capsid.

The amino acid compositions of the major capsid proteins of mengovirus have been determined (84). There are more acidic than basic amino acid residues, a small number of sulfur containing residues, and a large number of proline and non-alpha helix forming residues. These data are consistent with optical rotatory dispersion and circular dichroism measurements which indicate that few alpha helices are associated with the mengovirus capsid (39,71). The prevalence of acidic residues is supported by data which indicate that the the isoelectric points of the

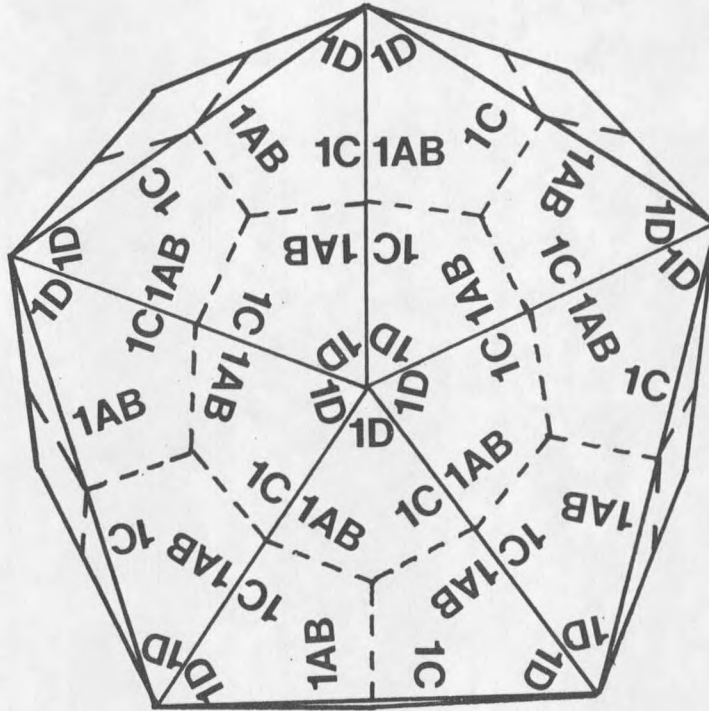


Figure 1. A model of the mengovirus capsid. The proposed arrangements of the epsilon (1AB), gamma (1C), and alpha (1D) proteins are shown prior to the cleavage of the epsilon (1AB) proteins to form the delta (1A) and beta (1B) proteins. This cleavage results in the formation of infectious mengovirus particles. The figure is modified from Rueckert (69) and Scraba (73).

major capsid proteins are acidic (15).

Protein Processing and Assembly of Virus Particles

In the initial stages of infection, mengovirus adsorbs to receptors on the cell surface, is internalized, and uncoated. The virion RNA functions as messenger RNA and is translated by the cell. Almost the entire length of the genome is translated from a single initiation site into a large precursor polypeptide from which both structural and nonstructural proteins are produced by enzymatic cleavage (64,69). The pattern of cleavage resulting in the generation of the mengovirus capsid proteins is shown in Figure 2. Primary cleavages of the nascent polypeptide generate the capsid polypeptide precursor, A (1-2A), and a precursor for proteins which are responsible for replication of the viral RNA, C (P3), and other nonstructural proteins. Primary cleavages are probably produced by cellular proteases (42). The capsid polypeptide precursor, A (1-2A), is thought to undergo an autocatalytic cleavage to form capsid precursor B (P1). Secondary cleavages of the capsid polypeptide precursor (P1) result in the generation of capsid proteins epsilon (1AB), gamma (1C), and alpha (1D). Secondary cleavages may be produced by both cellular and viral proteases (42,43). The cleavage of epsilon (1AB) to form the delta (1A) and beta (1B) capsid proteins occurs during the assembly of

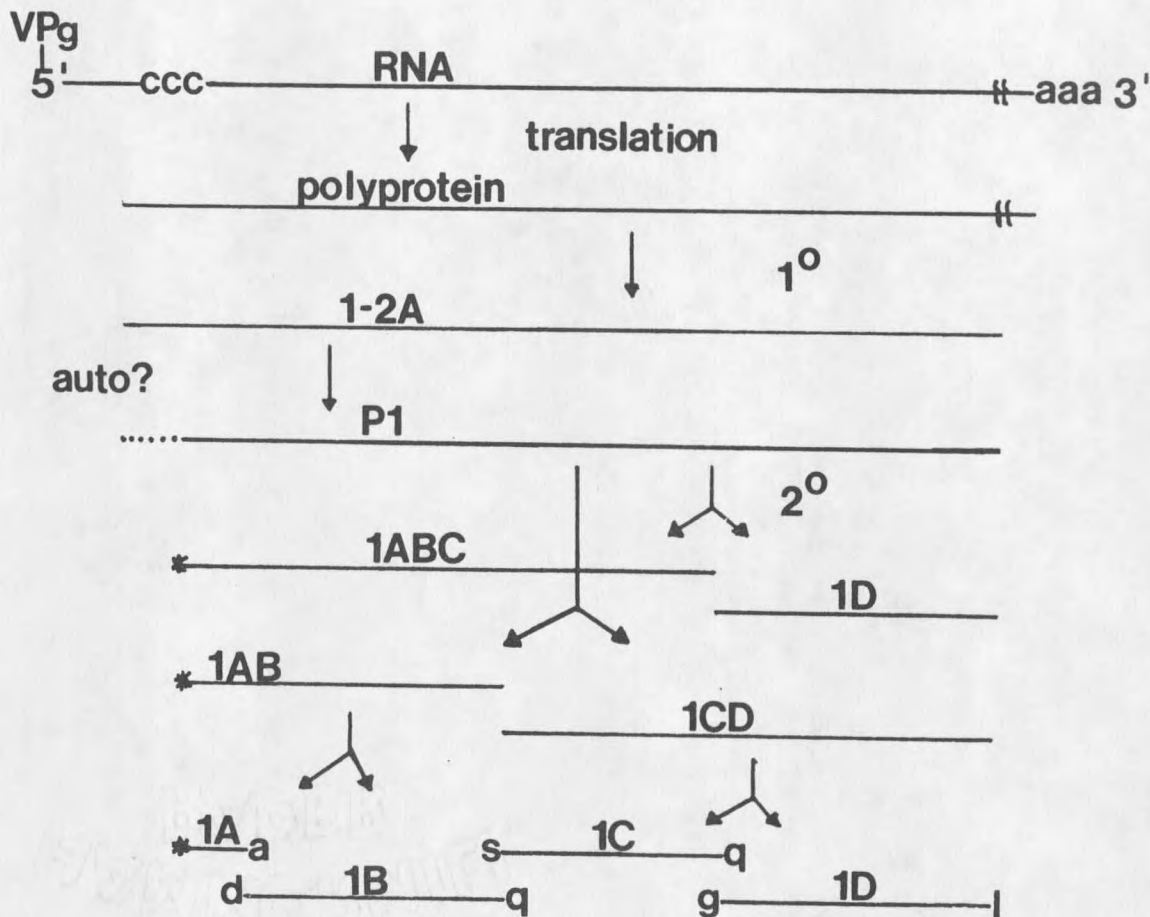


Figure 2. A diagram showing the generation of the capsid polypeptides of mengovirus. The genomic RNA contains a polycytidylate tract near the 5' end and a polyadenylate tract at the 3' end. The genome-linked protein is found at the 5' end of the molecule. The RNA is translated and precursor proteins are cleaved to form the capsid polypeptides by cellular and viral proteases as described in the text. The amino- and carboxyl-terminal amino acid residues of the capsid proteins are shown: *-blocked terminus, a-alanine, d-aspartate, q-glutamine, s-serine, g-glycine, and l-leucine. The figure is modified from Scraba (73).

the virion and most likely involves a viral protease. The amino- and carboxyl-terminal residues of each of the capsid proteins have been determined (85) and are shown in Figure 2. Secondary cleavages resulting in the generation of epsilon (1AB), gamma (1C), and alpha (1D) may be mediated by a protease with specificity for glutamine residues.

A mechanism for the assembly of mengovirus has been proposed (45). Five capsid protein precursors (P1) bind together and are subsequently cleaved to form a 14S subunit: (epsilon-gamma-alpha)₅ or (1AB-1C-1D)₅. Five of these 14S subunits aggregate to form 53S particles which dimerize to form 75S particles or incomplete capsids. Following the insertion of viral RNA into incomplete capsids, the virion matures by morphogenetic cleavage of epsilon (1AB) into delta (1A) and beta (1B) and the addition of two more 14S subunits. Uncleaved precursor proteins associated with the virions are thought to be contributed by the two 14S subunits which complete the assembly of virions.

Structure of the Virion

The spatial relationships among the mengovirus capsid proteins have been investigated by surface labeling of intact particles (46), reaction with polypeptide-specific antisera (46), and treatment of intact particles with

several different cross-linking reagents (35). ^{125}I labeling of the surface tyrosine residues of intact particles shows that the alpha (1D) and beta (1B) proteins are exposed on the surface of intact particles and that the delta (1A) and gamma (1C) proteins are located internally. Reaction of polypeptide-specific antisera with intact particles confirm these results (46). Anti-alpha (1D) sera, anti-beta (1B), and anti-alpha-beta sera (1D-1B) react with intact particles by immunodiffusion, whereas anti-delta (1A) and anti-gamma (1C) do not. Anti-alpha (1D) sera blocks the attachment of intact particles to cellular receptors, but anti-beta (1B) sera does not. Therefore, the surface determinants involved in attachment to cellular receptors may be associated with the alpha (1D) protein.

The asymmetric structural unit (protomer) of the mengovirus capsid is thought to be composed of one molecule each of alpha (1D), beta (1B), and gamma (1C) (49). The protomers are associated by hydrophobic interactions to form pentamers and 12 pentamers are associated by electrostatic interactions in the formation of capsids (35). The organization of the structural proteins has been elucidated by reaction of intact particles with bifunctional cross-linking reagents and analysis of the composition of the resulting complexes (35). The hydrophobic interaction, which results in

aggregation of five protomers to form a pentamer is a result of alpha-alpha (or 1D-1D) bonding. The electrostatic interactions which bind the pentamers together is a result of alpha-beta (or 1D-1B) bonding. Two models which demonstrate the protein bonding networks compatible with these data have been proposed (25). However, these models are incomplete in that they do not take into account the location of the delta (1A) proteins and two copies each of epsilon (1AB), D1 (1ABC), and D2 (1CD). Although the delta (1A) protein is lost upon elution of capsids which have attached to cellular membranes (19), it is thought to occupy an internal position in the capsid due to its lack of antigenicity in intact particles and because it is not recognized by surface labeling of intact particles with ^{125}I (46). Also, there is evidence which suggests that the delta (1A) protein can be cross-linked to virion RNA in the presence of ultraviolet light (55).

Pathogenic Properties

Mengoviruses have been isolated from several species of mosquitos, two rhesus monkeys, a mongoose, and a human (20). Mengovirus isolates were first demonstrated by their pathogenicity in mice (21). The isolates are pathogenic for mice when inoculated intracerebrally, intraperitoneally, intracranially, or subcutaneously.

Virus suspensions from early passages of the mengovirus isolates in mice kill most of the animals. Death is preceded by paralysis of one or more limbs. Adaptation of the virus by continuous passage through the brains of mice results in the production of a virus strain capable of killing mice in 24 to 48 h without visual symptoms of infection.

When lethal doses of mengovirus are inoculated intra-peritoneally, the virus appears first in the lymph nodes and spleen, followed by appearance in the brain and spinal cord (17). Titration of brain, spinal cord, spleen, kidney, liver, heart, and lung suspensions following intra-peritoneal inoculation indicates that mengovirus is most concentrated in the brain and spinal cord (21). Microscopic examination of these tissues indicates that the only discernible lesions are found in the brain and spinal cord. Nerve cell damage is evident in all parts of the brain. The most extensive damage is found in the hippocampus.

A strain of mengovirus has been isolated by plaque purification which, in addition to encephalitis, causes diabetes (82). Microscopic examination of pancreases of infected mice indicates the presence of viral antigens and necrosis of the islets of Langerhans.

Virus-Cell Interactions and Receptor Studies

Several different laboratories have investigated the molecular nature of virus-cell interactions involving both mengovirus and the closely-related EMC virus. Morishima et al. (56) have compared the genomic and receptor attachment differences between mengovirus and EMC virus. Although these viruses cannot be distinguished antigenically, biologically they are quite different. The EMC-D clone produces diabetes, but not encephalitis, whereas the mengovirus strain, 2T, produces a lethal encephalitis, but not diabetes. Twenty percent of the nucleotide sequences of the two viral genomes are different as estimated by thermoelution of cDNA-RNA hybrids. The rate of binding of mengovirus to neuronal cells is 5 to 10-fold greater than that of EMC-D. Receptor saturation experiments show that unlabeled virus fails to block the binding of heterologous virus. These data suggest that mengovirus and EMC virus bind to different receptors on the cell surface. The difference in tropism for neuronal and nonneuronal cells is reflected by the difference in pathogenicity between these two viruses.

Both mengovirus and EMC virus agglutinate human type O erythrocytes (26,28). Studies on hemagglutination by EMC virus have been focused on glycophorin, the major sialoglycoprotein found on human erythrocyte membranes (30,51).

Glycophorin can serve as a receptor for EMC virus (28,63). A specific sialoglycopeptide, isolated by chymotryptic digestion of glycophorin, has receptor-like properties for EMC virus (13). The entire peptide sequence and carbohydrate composition of glycophorin has been determined (78). However, very little is known about the nature of the determinants on the virus responsible for the binding of glycophorin.

Biological and Biochemical Properties of Plaque Variants

The biological, physical, and chemical properties of mengovirus have been investigated by the isolation and characterization of plaque size variants (2,26). Amako and Dales (2) have examined differences between L-mengo (large) and S-mengo (small) plaque variants. L-mengovirus induces rapid lysis and release of progeny. S-mengovirus lyses infected cells 3 to 5 h later, delaying the release of progeny. Virus-specified RNA synthesis begins at the same time period for both viruses. However, L-mengovirus RNA synthesis stops abruptly at an earlier time such that more RNA is produced by S-mengovirus. Thus, the virus yield per cell for S-mengovirus is 6- to 10-fold greater than that of L-mengovirus. The difference in plaque size between the variants is thought to be related to the rate of cell killing. Less than 20 plaque forming units (PFU) of L-mengovirus kill all infected mice 3 to 5 days after

intraperitoneal inoculation, whereas 4 logs more PFU of S-mengovirus are necessary to kill 90% of the mice within 8 days. Amako and Dales (2) speculate that a capsid protein synthesized late in infection may be responsible for the induction of cell lysis, upon which both virulence in mice and the plaque size of the variant are dependent.

Ellem and Colter (26) isolated three plaque size variants of mengovirus designated L-(large), M-(medium), and S-(small). These variants differ biologically with respect to rate of binding to cultured cells (18), sensitivity to low pH (18), and virulence in mice (17). The rate of binding of the L variant to L cells is much less than that of the M and S variants which bind L cells at similar rates. An increase in the pH of the virus-cell interaction from 6.8 to 8.0 increases the titer of the L, S, and M variants by 2-, 10-, and 3000-fold, respectively. The effect of pH is due, in part, to the instability of the M and S variants at pH values less than 7.2. The amount of virus able to kill 50% of the infected mice (LD_{50} titer) was determined (17). The L, M, and S variants all have LD_{50} titers of 1 to 5 PFU in mice infected intracerebrally. The L, M, and S variants have LD_{50} titers of 1, $1-5 \times 10^4$, and $2-10 \times 10^4$, respectively, in mice infected intra-peritoneally.

The physical and chemical properties of purified virions and RNAs of the L, M, and S variants of mengovirus

were compared. Analysis by electron microscopy, ultracentrifugation, optical rotatory dispersion (71), amino acid and nucleotide compositions (72), immunodiffusion (59), and isoelectric focusing (15) failed to detect any differences among the variants. The sole biochemical difference among these variants was detected by SDS-polyacrylamide gel electrophoresis (SDS-PAGE) (15). The M variant has a minor polypeptide component of 10 kd whereas, the L and S variants do not. The physical and chemical studies suggest that very minor differences in the physical and chemical composition may result in striking differences in the biological activities of mengovirus.

Temperature-Sensitive Mutants of Mengovirus

Temperature-sensitive mutants were isolated and characterized to examine the structural and biological properties of mengovirus. Twenty-four temperature-sensitive mutants have been characterized physiologically with respect to phenotype by Bond and Swim (4). Mutants were generated by treatment of virus-infected cells with N-methyl-N-nitro-N-nitrosoguanidine at a concentration which inhibits viral RNA synthesis by 75% and virus yield by 95%. Temperature-sensitive mutants were selected by replica plating of isolated plaques followed by incubation under permissive (31.5°C) and restrictive (39.5°C)

conditions. The mutants were separated into four groups on the basis of viral RNA synthesis: RNA^- , RNA^* , RNA^\pm and RNA^+ . Mutants which synthesized less than 25% of wild-type RNA synthesis at 39.5° were designated RNA^- . Mutants which exhibited alterations in RNA synthesis at 31.5 and 39.5°C were designated RNA^* . Other mutants were divided into two groups, RNA^\pm (25 to 49% of wild-type RNA synthesis) and RNA^+ (50 to 100% of wild-type RNA synthesis).

Reciprocal temperature-shift experiments were performed to examine physiological changes resulting from infection by the RNA^- mutants. One mutant expresses a defect at the beginning of RNA synthesis. Three mutants express defects before the start of RNA synthesis and may be defective in translating the infecting RNA or in protein processing. Polymerase synthesized at 31.5°C by the RNA^- mutants is active at 39.5°C . Therefore, mutations in the polymerase resulting in defective RNA synthesis are unlikely.

Temperature-shift experiments performed with the RNA^\pm and RNA^+ mutants indicate that the temperature-sensitivity of most of these mutants extends throughout the replicative cycle. However, four of the mutants exhibit temperature-sensitive defects in the first HPI. Therefore, an early event may be required for the maturation of virions.

The composition and thermostability of wild-type

mengovirus and several temperature-sensitive mutants were examined (5). The virions of two thermolabile, temperature-sensitive mutants contain an increased amount of the beta' (1B') protein, coupled with a corresponding decrease in the amount of beta (1B) protein. These data suggest that alterations of the proteolytic cleavage of the beta (1B) protein may result in increased thermolability of virus particles. These data are consistent with the data of Hordern et al. (35) which indicate that the beta (1B) protein is involved in bonding of the 14S pentameric subunits of the capsid.

Eleven temperature-sensitive mutants of mengovirus have been isolated and partially characterized (Dr. M. A. Gill, personal communication). The mutants were generated by treatment of virus-infected cells with 10 ug/ml of acriflavin at 5.75 HPI. This concentration inhibits viral RNA synthesis by 80% and virus yield by 99%. The mutants were selected by temperature-shift analysis of isolated plaques on L929 cell monolayers. Infected-cell monolayers were incubated at 31.5°C until plaques were evident. The plaques were measured, incubated at 39.5°C for 24 h, and remeasured. Those plaques which did not increase in size at 39.5°C were considered to be temperature-sensitive and selected for further analysis.

The eleven temperature-sensitive mutants were characterized by their ability to synthesize RNA at 39.5°C

and agglutinate human type O erythrocytes. The mutants were grouped by the convention of Bond and Swim (4). The results are shown in Table 1. Eight of the mutants are RNA⁺, two RNA⁻, and one RNA⁺. Two of the RNA⁺ mutants, 205 and 280, do not agglutinate human type O erythrocytes.

Since mutants 205 and 280 are not defective in synthesizing viral RNA at the restrictive temperature, 39.5°C, and do not agglutinate human type O erythrocytes, it is likely that a defect in the structural proteins of these mutants would account for their differences in biological function with respect to the wild-type virus. Therefore, these mutants would be excellent candidates for further studies which relate alterations of the structure

Table 1. Characterization of temperature-sensitive mutants of mengovirus with respect to RNA synthesis and hemagglutination.

Mutant	RNA synthesis ^a at 39.5°	Hemagglutination activity
205	+	-
217	+	+
218	+	+
223	+	+
228	+	+
237	+	+
241	-	+
243	+	+
275	+	+
277	+	+
280	+	-

^a The grouping of mutants with respect to RNA synthesis was done by the convention of Bond and Swim (4).

of the mengovirion to changes in biological activities of these mutants.

I chose to compare the biological and structural properties of the mengovirus mutants, 205 and 280, with those of the wild-type virus. This study was designed to elucidate the mechanism of interaction of mengovirus with erythrocytes during hemagglutination and the biological consequences of mengovirus infection in mice. Revertants which express alterations in virulence were isolated from mutant infected mice and characterized. The structure of the wild-type and mutant virions radiolabeled by metabolic or surface labeling were analysed by SDS-PAGE, peptide mapping, and two-dimensional gel electrophoresis. Physiological changes associated with virus-specified macromolecular synthesis in mutant and revertant virus-infected cells were also examined.

MATERIALS AND METHODS

Chemicals and Reagents

Reagent grade liquid organic chemicals were obtained from J. T. Baker Chemical Co. Other chemicals and reagents were obtained from Sigma Chemical Co. unless otherwise stated in the text. Radioisotopes were obtained from New England Nuclear Corp.

Virus Strains

The wild-type strain of mengovirus was obtained from Dr. H. E. Swim and has been previously described (4,5). This strain, designated 37A, was derived from eight consecutive passages of heat stable variants in L cells in the laboratory of Dr. A. F. Graham (9). Mutants of mengovirus were isolated from cells infected with virus in the presence of either N-methyl-N'-nitro-N-nitrosoguanidine (ts25) by Bond and Swim (4) or acriflavine (ts205, ts237 and ts280) by Dr. M. A. Gill (personal communication). Mengovirus mutants were cloned twice from plaque isolates and virus stocks were prepared by subsequent infection of BHK-21 cells at a multiplicity of infection (MOI) of 0.1 plaque forming units (PFU) per cell.

Cell Lines

The BHK-21 cell line used routinely in the propagation and assay of wild-type and mutant strains of mengovirus was obtained from Dr. J. J. Holland. This spontaneously transformed continuous cell line was derived from the kidneys of one-day-old hamsters (47).

Several murine cell lines were examined as hosts for mengovirus multiplication and adsorption. 17CL-1 cells are a spontaneously transformed continuous cell line cloned from 3T3 fibroblasts derived from BALB/c mice and were obtained from Dr. L. S. Sturman (76). L-929 cells [American Type Culture Collection (ATCC), CCL 1] are a cloned spontaneously transformed continuous cell line derived from C3H/An mice. Neuro-2A cells are a continuous cell line derived from Cl300 tumor cells isolated from strain A mice and were obtained from Dr. C. Miller (41). NB41A3 cells (ATCC, CCL 147) were derived from a clone of the Cl300 tumor cells.

Sarcoma-180 cells (ATCC, TIB 66) were used to produce ascitic fluid in BALB/c mice. This cell line was derived from Swiss Webster mouse ascitic tumor cells.

Cells were maintained in Dulbecco's Modified Eagle's medium (Irvine Scientific) (24) containing 4.5 g/l glucose (designated DME 0) and 10% (vol/vol) calf serum (Sterile Systems) (designated DME 10). Virus stocks were produced

by infecting BHK-21 cells at an MOI of 0.1 in DME 2, which is DME 0 supplemented with 2% (vol/vol) fetal bovine serum (Sterile Systems), 10 mM 3-(N-morpholino)propanesulfonic acid (MOPS), 10 mM N-tris-(hydroxymethyl)methyl-2-aminoethanesulfonic acid (TES), and 10 mM N-2-hydroxyethyl-piperazine-N'-2-ethanesulfonic acid (HEPES). Infected cell lysates were frozen at -70°C , thawed, and clarified by centrifugation in a HB-4 rotor at $2000 \times g$ for 10 min at 4°C .

Plaque Assay

Virus stocks were titered by plaque assay on BHK-21 cell monolayers. Cells (1×10^6) were seeded into plastic six-well dishes (Linbro) in DME 10 and incubated at 37°C overnight. Monolayers were washed with pre-warmed DME 0 and infected with 0.2 ml of 10-fold dilutions of virus in DME 2. Dilutions of virus were allowed to adsorb to the monolayers for 60 min at room temperature. The medium was aspirated and the monolayers were overlaid with 2 ml of DME 2 containing 0.75% (wt/vol) agarose (type II, Sigma), and incubated at 33°C for 48 h. Cells were fixed by adding 0.5 ml of 2% (vol/vol) glutaraldehyde to each dish followed by incubation for 60 min at 33°C . The agarose overlay was removed and the cells were stained with 1 ml of 0.4% (wt/vol) crystal violet, 20% (vol/vol) ethanol for 30 min at room temperature. The stained monolayers were

washed extensively with water, dried at room temperature and the plaques were counted. Data were expressed as PFU/ml of the titered virus suspension.

Infection and Purification

Cells were infected with virus in suspension or monolayers of cells were infected. Cells suspended in DME 2 (1×10^7 cells/ml) were infected with virus at an MOI of 3 and incubated at 33°C for 30 min. Following adsorption, cells were centrifuged for 5 min at $500 \times g$, resuspended in DME 2, and plated into plastic 10 cm dishes. Virus-infected cells were incubated at 33°C until lysis, then frozen at -70°C . Alternatively, monolayers were overlaid with virus and incubated at 33°C for 30 min. The medium was aspirated, replaced with DME 2, and the cells were incubated at 33°C until lysis, then frozen at -70°C .

To purify virus, lysates were thawed, pooled and clarified by centrifugation in an HB-4 rotor at $4000 \times g$ for 15 min at 15°C . Sodium dodecyl sulfate (SDS) was added to the supernatant fluid to 0.2% (wt/vol) which was then reclarified as above. The resulting supernatant fluid was layered over a pad of 28% (wt/wt) sucrose in Bu3 [10 mM Tris-HCl (pH 7.4), 10 mM EDTA, 50 mM NaCl], centrifuged in either an SW41 rotor at 37,000 rpm for 90 min or an SW27 rotor at 27,000 rpm for 150 min at 15°C . Pellets were resuspended in Bu3, layered onto 15-28% (wt/wt) sucrose

gradients in Bu₃, and centrifuged in an SW41 rotor at 35,000 rpm for 105 min at 6°C. Gradients were fractionated and virus was detected by either absorbance at 260 nm or monitoring radioactivity by liquid scintillation counting. Peak fractions were pooled, diluted with Bu₃, and centrifuged in an SW50.1 rotor at 43,000 rpm for 90 min at 6°C. Pellets were resuspended in TE buffer [10 mM Tris-HCl (pH 7.4), 10mM EDTA], layered onto a 27-42% (wt/wt) CsCl gradient in TE buffer, and centrifuged in an SW41 rotor at 33,000 rpm for 10 h at 6°C. Gradients were fractionated and virus was detected as described above. Peak fractions were pooled, dialyzed extensively against TE buffer, and the virions were pelleted by centrifugation in an SW50.1 rotor at 43,000 rpm for 90 min at 6°C.

Radiolabeling of Virus-Specified Proteins

Purified virions radiolabeled in vivo with L-[³⁵S]-methionine (NEG-009T) or [¹⁴C(U)]-L-amino acid mixture (NEC-445) were prepared as follows. Cells were infected at an MOI of 3 to 5 in DME 2 and incubated at 33°C. At 5.5 HPI (for the wild-type strain) or 6.5 HPI (for the mutant strains), the medium was aspirated from the virus-infected cells and replaced with either ¹⁴C-labeling medium or ³⁵S-labeling medium. The ¹⁴C-labeling medium contained 20% of the normal concentration of amino acids in DME 2 and 6 uCi/ml ¹⁴C-amino acid mixture. The ³⁵S-labeling medium

contained 20% of the normal concentration of methionine in DME 2 and 50 uCi/ml ^{35}S -methionine. The virus-infected cells were subsequently incubated at 33°C and labeled virions were purified from infected cell lysates as described above.

Surface tyrosine residues of purified virions were labeled with [^{125}I]-sodium iodide (NEZ-033H) using a modification of the method described by Millar and Smith (54). Pellets containing purified virions were resuspended in TN buffer [50 mM Tris-HCl (pH 7.5), 150 mM NaCl] and quantitated by adsorbance at 260 nm as described (69). Suspensions of purified virus in TN buffer containing 0.3 absorbance units (260 nm), 200 uCi of ^{125}I , and 100 ug of Iodogen (Pierce) (52) were added to Eppendorf centrifuge tubes (0.5 ml volume) in a total volume of 0.3 ml. The tubes were capped, inverted, and agitated for 10 min. An equal volume of 0.4 uM NaI, 5.0 uM 2-mercaptoethanol was added to each tube and the mixture was passed through Sephadex G-25 columns (60 x 7 mm) equilibrated with TN buffer. The excluded volumes were collected and centrifuged in an SW41 rotor at 37,000 rpm for 90 min at 6°C . Pellets were prepared for preparative SDS-polyacrylamide gel electrophoresis (SDS-PAGE).

Virus-specified intracellular proteins were labeled with L- [^{35}S]-methionine, immunoprecipitated with virus-specified hyperimmune ascitic fluid and SDS-PAGE. Cells

were mock-infected or infected with virus in suspension (1×10^7 cells/ml) at an MOI of 3, adsorbed, plated into plastic 35 mm dishes (2.5×10^6 cells/dish), and incubated at 33°C . The medium was aspirated from the virus-infected and mock-infected cells, replaced with 1.0 ml of methionine-free DME 2, and incubated for 10 min. Cells were labeled with 0.3 ml methionine-free DME 2 containing 100 $\mu\text{Ci/ml}$ ^{35}S -methionine for 15 min. The labeling medium was aspirated and the cells were washed twice with ice-cold DME 0. Cells were lysed with 0.1 ml B10 [10 mM Tris-HCl (pH 7.4), 5 mM MgCl_2 , 0.5% (vol/vol) NP40, 0.1% (wt/vol) SDS, 1% (vol/vol) Aprotinin, 50 $\mu\text{g/ml}$ ribonuclease A, 50 $\mu\text{g/ml}$ deoxyribonuclease] for 5 min on ice. Cellular lysates were centrifuged at $6,500 \times g$ for 1 min at 4°C and the supernatant fluid was collected and stored at -20°C .

Cytoplasmic lysates were immunoprecipitated by a modification of the procedure of Bond et al. (6). Cytoplasmic lysates representing 1.25×10^6 cells were diluted ten-fold in B11 [50 mM Tris (pH 7.4), 150 mM NaCl, 5 mM EDTA, 0.02% (wt/vol) sodium azide, 0.05% (vol/vol) NP40, 1% (vol/vol) Aprotinin, 0.1% (wt/vol) bovine serum albumin]. Twelve μl of mouse anti-mengovirus hyperimmune ascitic fluid was added to the lysates and incubated at 0°C for 60 min. Immune complexes were precipitated with 100 μl of 10% (vol/vol) fixed Staphylococcus aureus (Cowan

